Supporting Information

Molecular Tetrominoes: Selective Masking of Donor π-Face to Control Configuration of Donor-Acceptor Complex

Jenna L. Sartucci, Arindam Maity, Manikandan Mohanan, Jeffery Bertke, Miklos Kertesz, and Nagarjuna Gavvalapalli*

Department of Chemistry, Institute for Soft Matter Synthesis and Metrology, Georgetown University, 3700 O St NW, Washington, D.C., 20057, USA.

Table of Contents

General Information

Unless otherwise stated, reactions were performed in oven-dried glassware fitted with rubber septa under nitrogen atmosphere and were stirred with Teflon-coated magnetic stirring bars. Reagents used for the synthesis were purchased from Fisher, Acros, Alfa Aesar and Sigma Aldrich. All air or moisture-sensitive reactions were performed under nitrogen atmosphere using standard Schlenk techniques. Thin layer chromatography was performed using Silica gel 60 F-254 precoated plates (0.25 mm) and visualized by UV irradiation or $KMnO_4$ stain. Silica gel of particle size 230-400 mesh was used for flash chromatography. Unless otherwise stated, all starting materials and reagents were used without further purification. ^1H and ^{13}C spectra were recorded on Varian 400-MR NMR. Chemical shifts are reported in δ (ppm) relative to the residual solvent peak $CDCl_3$: 7.26. Coupling constants (J) are expressed in Hertz (Hz). Splitting patterns are designated as s(singlet), br(broad signal), d(doublet) and t(triplet). High resolution TOF MS EI+ mass spectra were recorded in the Mass Spectrometry laboratory, School of Chemical Sciences at University of Illinois Urbana-Champaign. UV-vis absorption spectra were recorded on Agilent Technologies Cary Series 5000 UV-vis-NIR Spectrophotometer.

Synthesis

PCP((±)-9)

A round bottom flask was charged with compound 6a[1-3] (1.43 mmol), CuI (0.143 mmmol), and $Pd(PPh_3)_4$ (0.143 mmol) under nitrogen and sealed. Deoxygenated piperidine was added (100 mL) followed by phenyl acetylene (4.3 mmol). The reaction stirred under nitrogen for 4 hours at 80˚ C. Upon completion, solvent was removed under reduced pressure and the crude mixture was adsorbed onto silica for flash column chromatography with an eluent of 20% dichloromethane in hexanes. Purification yielded a white powder in 66% yield. **^{1}H NMR** (400 MHz, CDCl3) δ: -0.18- 0.1 (d, 2H), 0.8- 1.25 (d, 8H), 1.35- 1.5 (bs, 4H), 1.8- 1.95 (bs, 2H), 2.66 (bs, 2H), 3.4- 3.6 (m, 2H), 4.0- 4.5 (d, 2H), 7.38 (m, 7H), 7.56 (m, 5H). **^{13}C NMR** (100 MHz, $CDCl_3$) δ: 31.6, 36.5, 37.7, 39.2, 39.7, 40.2, 41.4, 45.5, 47.3, 90.4, 97.6, 125.6, 125.9, 126.7, 131.1, 131.3, 134.2,

136.4, 137.3, 145.2, **HRMS** (TOF MS EI) m/Z 530.2090 [M]+; calculated for [$C_{36}H_{34}S_2$]: 530.2102.

CPC ((±, meso)-10)

A round bottom flask was charged with compound (±)-8[1-3] (0.56 mmol), CuI (0.026 mmol), and Pd(^{t}Bu$_3$P)$_2$ (0.026 mmol) under nitrogen and sealed. Deoxygenated piperidine was added (15 mL) followed by iodobenzene (0.26 mmol). The reaction stirred under nitrogen for 2 hours at room temperature. Upon completion, solvent was removed under reduced pressure and the crude mixture was adsorbed onto silica for flash column chromatography with an eluent of 35% dichloromethane in hexanes. Purification yielded a white powder in 69% yield. **^{1}H NMR** (400 MHz, CDCl3) δ: -0.35- 0.0 (m, 4H), 0.75- 1.0 (m, 4H), 1.13 (bs, 8H), 1.42 (s, 8H), 1.82 (bs, 2H) 1.9 (s, 5H), 2.22 (d, 1H), 2.65 (bs, 4H), 3.35- 3.61 (m, 4H), 3.73 (m, 2H), 4.12 (d, 1H), 4.35 (d, 1H), 7.11 (d, 2H), 7.27- 7.46 (m, 3H), 7.55 (s, 4H), 7.61 (s, 1H). **^{13}C NMR** (100 MHz, CD_2Cl_2) δ: 29.2, 33.9, 35.3, 36.5, 38.2, 38.8, 42.8, 44.6, 89.9, 93.1, 94.7, 123.5, 131.0, 131.6, 133.5, 134.2, 141.2, 143.0, **HRMS** (TOF MS EI+): 782.3097 m/Z $[M]^+$; calculated for $[C_{50}H_{54}S_4]^+$: 782. 3108.

Scheme S1: General Reaction Scheme for the Synthesis of PLP (12):

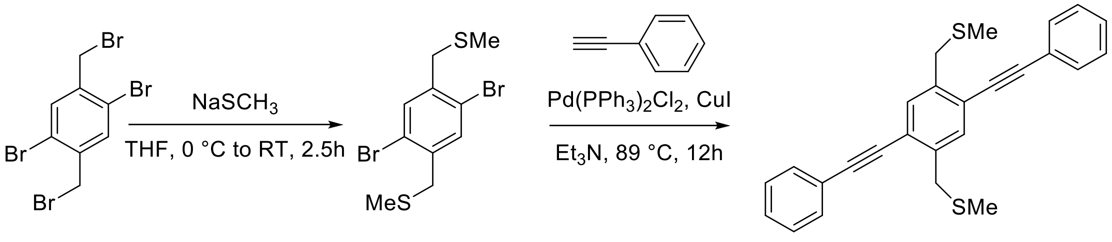

(**11**)

(**12**)

PLP

Synthesis of ((2,5-dibromo-1,4-phenylene)bis(methylene))bis(methylsulfane) (11):

The Synthesis of ((2,5-dibromo-1,4-phenylene)bis(methylene))bis(methylsulfane) was performed using a known procedure from literature.[4] In an oven-dried round-bottom flask 1,4-dibromo-2,5-bis(bromo methyl)benzene (2 g, 4.74 mmol, 1.0 equiv.) was taken in THF (60 ml) under nitrogen. The reaction vessel was kept in an ice bath maintaining 0 ˚C. Sodium thiomethoxide (997 mg, 14.228 mmol, 3.0 equiv.) was added pinch by pinch to the solution. The milky white suspension was stirred at room temperature for 2.5 h. After completion of the reaction (judged by TLC), the reaction mixture was poured into water (300 ml) and the product was extracted with dichloromethane (3 X 120 ml). The combined organic extracts were dried over anhydrous Na_2SO_4 and concentrated in a rotary evaporator. The crude mixture was purified by flash column chromatography (using 5% EtOAc in hexane) to afford compound **11** as a white solid. (1.4 g, 83% yield). R_f = 0.45 (10% EtOAc in hexane). **^{1}H NMR** (400 MHz, $CDCl_3$) δ: 7.56 (s, 2H), 3.74 (s, 4H), 2.08 (s, 6H). **^{13}C NMR** (100 MHz, $CDCl_3$) δ: 140.88, 137.16, 125.85, 40.41, 17.97. **HRMS** (TOF MS EI$^+$): 353.8743 m/Z $[M]^+$; calculated for $[C_{10}H_{12}Br_2S_2]^+$: 353.8747.

Synthesis of PLP (12):

An oven dried round bottom flask was charged with compound 2,5-dibromo-1,4-phenylene)bis(methylene))bis(methylsulfane) (100 mg, 0.281 mmol, 1.0 equiv.), $Pd(PPh_3)_2Cl_2$ (9.8 mg, 0.0145 mmol, 5 mol%) and CuI (1 mg, 0.0056 mmol, 2 mol%) under nitrogen and sealed. Deoxygenated Triethylamine (4 ml) was added under nitrogen followed by Phenyl acetylene (.123 ml, 1.123 mmol, 4.0 equiv.). The brownish solution was set to reflux for 12h. Upon completion (judged by TLC), solvent was removed under reduced pressure and the crude mixture was diluted with dichloromethane (3 ml). The dichloromethane layer was washed with brine (1 ml), dried over anhydrous Na_2SO_4 and concentrated under vacuum. The residue was further purified by flash column chromatography (using 4% EtOAc in hexane) to afford PLP trimer as a white solid. (72 mg, 65% yield). R_f = 0.40 (5% EtOAc in hexane). **^{1}H NMR** (400 MHz, CD_2Cl_2) δ 7.60 – 7.57 (m, 6H), 7.44 – 7.39 (m, 6H), 3.93 (s, 4H), 2.12 (s, 6H). **^{13}C NMR** (100 MHz, CD_2Cl_2) δ 141.86, 135.43, 134.14, 131.33, 131.14, 125.61, 125.58, 98.32, 89.93, 38.74, 17.71. **HRMS** (TOF MS EI$^+$): 398.1157 m/Z $[M]^+$; calculated for $[C_{26}H_{22}S_2]^+$: 398.1163.

Scheme S2: General Reaction Scheme for the Synthesis of LPL (14):

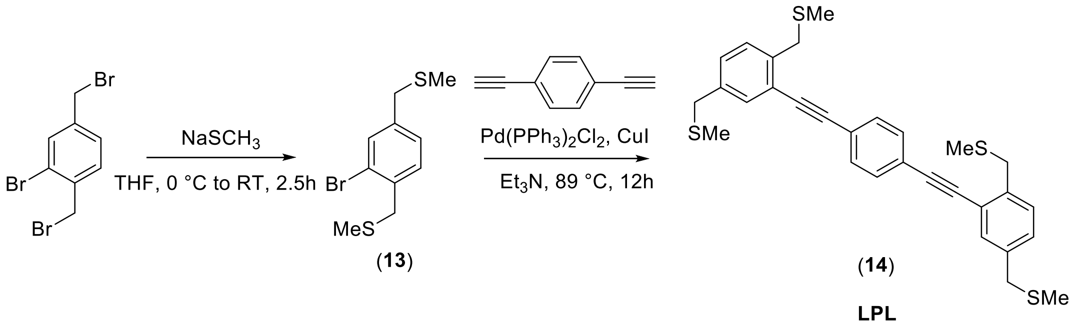

Procedure for the Synthesis of ((2-bromo-1,4-phenylene)bis(methylene))bis(methylsulfane) (13):

Compound **13** was synthesized from 2-bromo-1,4-bis(bromomethyl)benzene following the same procedure used for compound **11**. The compound **13** was obtained as a colorless liquid (1.37 g, 85% yield). R$_f$ = 0.45 (10% EtOAc in hexane). **^{1}H NMR** (400 MHz, CDCl$_3$) δ: 7.52 (s, 1H), 7.30-7.28 (d, *J* = 7.8 Hz, 1H), 7.22-7.20 (d, *J* = 7.8 Hz, 1H), 3.79 (s, 2H), 3.61 (s, 2H), 2.06 (s, 3H), 2.00 (s, 3H). **^{13}C NMR** (100 MHz, CDCl$_3$) δ: 141.79, 138.85, 135.90, 133.31, 130.51, 127.10, 40.76, 40.07, 17.86, 17.69. **HRMS** (TOF MS EI$^+$): 375.9648 m/Z [M]$^+$; calculated for [C$_{10}$H$_{13}$BrS$_2$]$^+$: 375.9642.

Procedure for the Synthesis of LPL (14):

Trimer LPL was synthesized from compound **13** following the same procedure used for compound **12**. The compound **14** was obtained as a white solid (246 mg, 43% yield). R$_f$ = 0.35 (10% EtOAc in hexane). **^{1}H NMR** (400 MHz, CD$_2$Cl$_2$) δ 7.58 (s, 4H), 7.52 (s, 2H), 7.37-7.35 (d, *J* = 7.7 Hz, 2H), 7.32-7.30 (d, *J* = 7.5 Hz, 2H), 3.94 (s, 4H), 3.69 (s, 4H), 2.10 (s, 6H), 2.04 (s, 6H). **^{13}C NMR** (100 MHz, CD$_2$Cl$_2$) δ 141.93, 140.18, 135.17, 134.12, 132.09, 131.92, 125.82, 125.28, 96.31, 92.17, 40.28, 38.96, 17.65, 17.42. **HRMS** (TOF MS EI$^+$): 518.1222 m/Z [M]$^+$; calculated for [C$_{30}$H$_{30}$S$_4$]$^+$: 518.1230.

Single Crystal X-Ray Diffraction

Single crystals of each compound **PCP ((±)-9)** (CCDC 2085842), **CPC ((±, meso)-10)** (CCDC 2085840), and **PPP-DDQ** (CCDC 2085841) were mounted under mineral oil on a Mitegen micromount and immediately placed in a cold nitrogen stream at 100(2) K prior to data collection. Data for compounds **PPP-DDQ** and **PCP** were collected on a Bruker D8 Quest equipped with a Photon100 CMOS detector and a Mo ImS source. Data for compound **CPC** was collected on a Bruker DUO equipped with an APEXII CCD detector and Mo fine-focus sealed source. A series of phi and omega scans were collected using monochromatic Mo Kα radiation, (λ = 0.7107 Å), and integrated with the Bruker SAINT[5] program. Structure solutions and refinements were performed using the SHELX suite[6] and SHELXLE.[7] Non-hydrogen atoms were refined with anisotropic thermal parameters. Further comments on structural models: $C_{50}H_{54}S_4$ (**CPC;** CCDC 2085840). A structural model consisting of the target molecule was developed. H atoms were included as riding idealized contributors. H atom U's were assigned as 1.2 times carrier U_{eq}. This crystal was refined as a pseudo-merohedral twin. The twin law by rows was (100) (0-10) (00-1). The ratio of the two twin domains refined to approximately 67:33. $C_{38}H_{14}Cl_{4}N_4O_4$ (**PPP-DDQ;** CCDC 2085841). A structural model consisting of one quinone molecule and one half of the triphenyl molecule per asymmetric unit was developed. The quinone molecule is disordered over two orientations. The like C-C, C-N, C-O, and C-Cl distances were restrained to be similar (esd 0.01 Å). Similar displacement amplitudes (esd 0.01) were imposed on disordered sites overlapping by less than the sum of van der Waals radii. H atoms were included as riding idealized contributors. H atom U's were assigned as 1.2 times carrier U_{eq}. $C_{36}H_{34}S_2$ (**PCP;** CCDC 2085842). A structural model consisting of the target molecule was developed. H atoms were included as riding idealized contributors. H atom U's were assigned as 1.2 times carrier U_{eq}. The absolute configuration could not be reliably determined. The model was refined as an inversion twin with the BASF parameter refining to 0.45.

Table 1. Crystal data and structure refinement for **PCP, CPC, and PPP-DDQ**.

	CPC	**PPP-DDQ**	**PCP**
Empirical formula	$C_{50}H_{54}S_4$	$C_{38}H_{14}Cl_{4}N_4O_4$	$C_{36}H_{34}S_2$
Formula weight	783.17	732.33	530.75
Wavelength/ Å	0.71073	0.71073	0.71073
Crystal system	Triclinic	Triclinic	Orthorhombic
Space group	P-1	P-1	$P2_12_12_1$
a/Å	9.185(7)	6.4871(13)	11.8779(6)

b/Å	12.053(9)	7.1989(15)	14.0953(7)
c/Å	19.519(14)	17.900(4)	16.4691(7)
α/deg	76.378(12)	92.211(8)	90
β/deg	89.717(12)	97.288(8)	90
γ/deg	89.993(13)	102.060(7)	90
Volume/Å^3	2100(3)	809.1(3)	2757.3(2)
Z	2	1	4
dcalc/g cm^{-3}	1.239	1.503	1.279
Absorption coefficient/mm^{-1}	0.261	0.416	0.217
Max./min. transmission	0.7452/0.5612	0.99019/0.91231	0.96301/0.95117
Size/mm	0.330 x 0.130 x 0.034	0.312 x 0.204 x 0.036	0.331 x 0.322 x 0.299
Reflections collected	35103	44132	172579
Independent reflections	7687	3310	6860
Parameters refined	489	353	344
R(int)	0.2698	0.0589	0.0288
Goodness-of-fit on F^2	1.033	1.074	1.108
R1, wR2 [I > 2σ(I)]	0.1047, 0.2080	0.0327, 0.0816	0.0335, 0.0900
R1, wR2 (all data)	0.2140, 0.2547	0.0428, 0.0877	0.0337, 0.0901
Largest peak, hole/ e Å^{-3}	0.449, -0.554	0.182, -0.192	0.493, -0.256

Spectroscopy

General

UV-Vis spectra of the charge transfer compounds were taken on a Cary Series 5000 UV-Vis-NIR at a concentration of 5 mM (for both the donor and acceptor) in Chloroform, unless otherwise stated. The spectra were normalized for the charge transfer peak in the visible region. Absorption spectra of just the donor molecules and DDQ were recorded in Chloroform at a concentration of 10 μM. All samples were measured at room temperature.

Fourier Transform Infrared Spectroscopy

FTIR measurements were taken on a Perkin Elmer IR with an ATR attachment. Samples were prepared in Chloroform or THF at a concentration of 5 mM (in each the donor and acceptor).

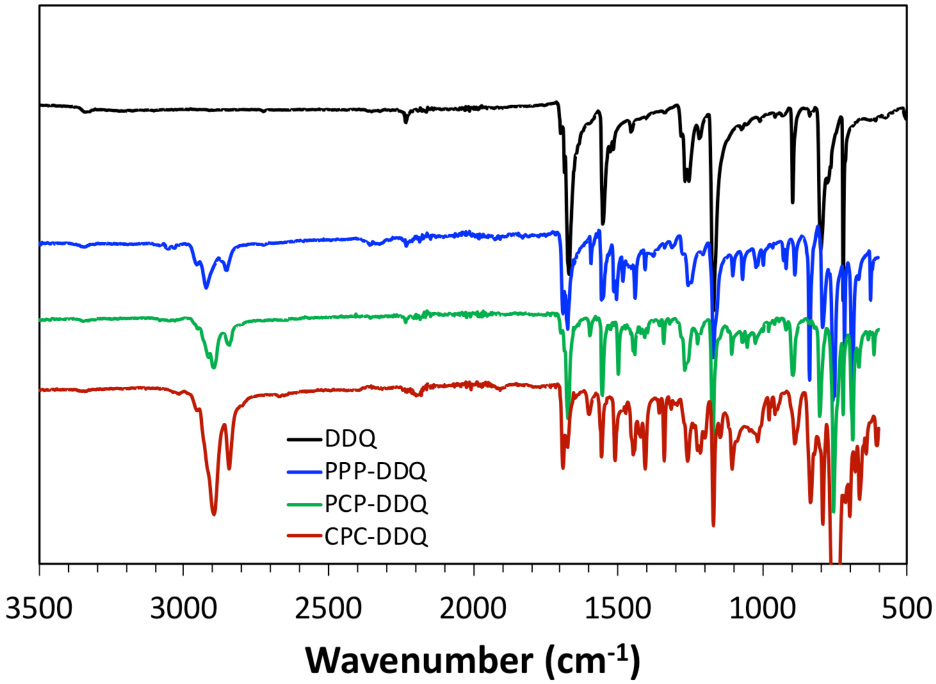

Figure S1. Full IR spectrum for DDQ (black), PPP-DDQ (blue), PCP-DDQ (green), and CPC-DDQ (red). Samples were prepared in chloroform and dried with a stream of Nitrogen followed by high vacuum.

Samples were dried with a concentrated stream of nitrogen followed by high vacuum. The films were scratched into a powder and loaded onto the ATR crystal for analysis.

Charge Transfer UV-Vis

The full spectra for each DA complex is show in Figure S2. The solutions were 5 mM each in both the donor and acceptor, hence the saturation in the UV region.

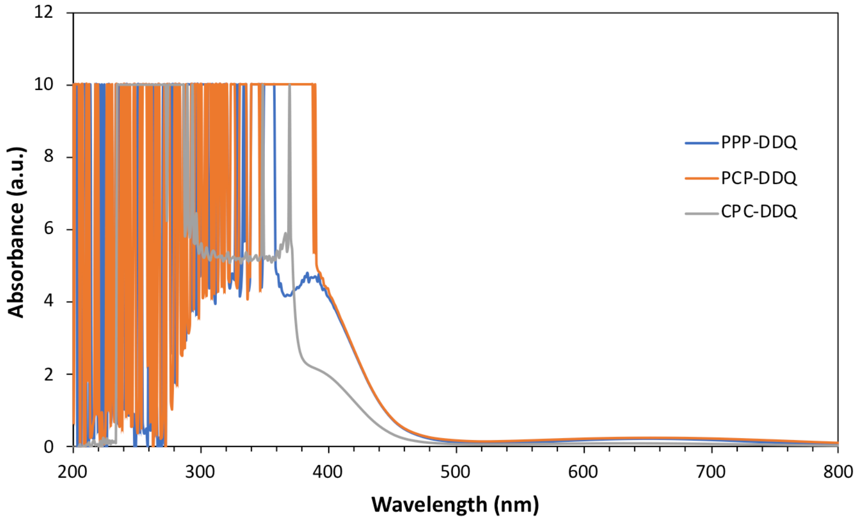

Figure S2. UV-vis absorption spectra of DA complex recorded in chloroform.

Charge Transfer Stoichiometry

The stoichiometry of the donor acceptor charge transfer complexes was measured using the method of continuous variation using the Job's Plot. Solutions were made with varying mole fractions of D:A and the absorbance of the CT peak was measured at each mole fraction. Samples were prepared with D:A ratios of 1:9, 2:8, 3:7, 4:6, 5:5, 6:4, 7:3, 8:2, 9:1. All samples were prepared in Chloroform and measured at room temperature.

Figure S3. Job's Plot for PCP-DDQ in chloroform. The stoichiometry of this charge transfer complex is 1:1.

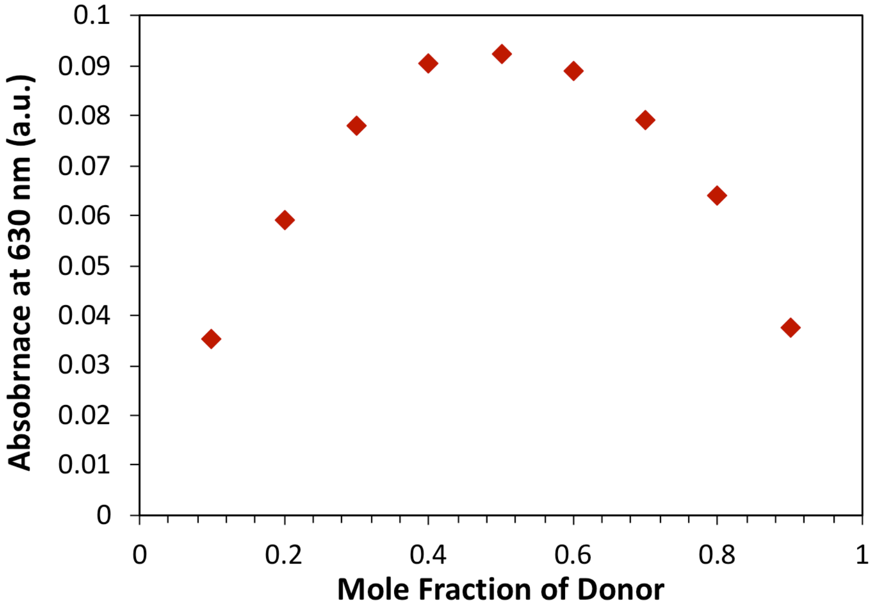

Figure S4. Job's Plot for CPC-DDQ in chloroform. The stoichiometry of this charge transfer complex is 1:1.

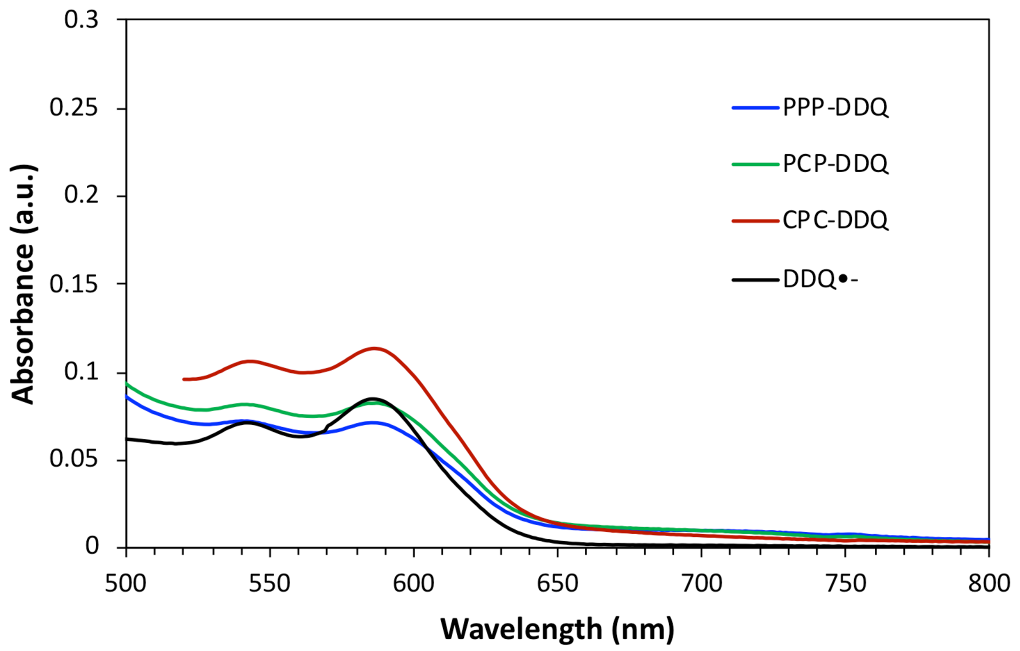

Figure S5. UV-vis absorption spectra of DA complexes measured in THF at room temperature.

Equation used to determine the percent increase in DDQ ionization relative to PPP-DDQ complex:

$$\%\text{ increase in DDQ ionization} = \frac{\text{Abs}_{\text{strapped DA}}\text{ at 590 nm} - \text{Abs}_{\text{PPP-DDQ}}\text{ at 590 nm}}{\text{Abs}_{\text{PPP-DDQ}}\text{ at 590 nm}} \times 100$$

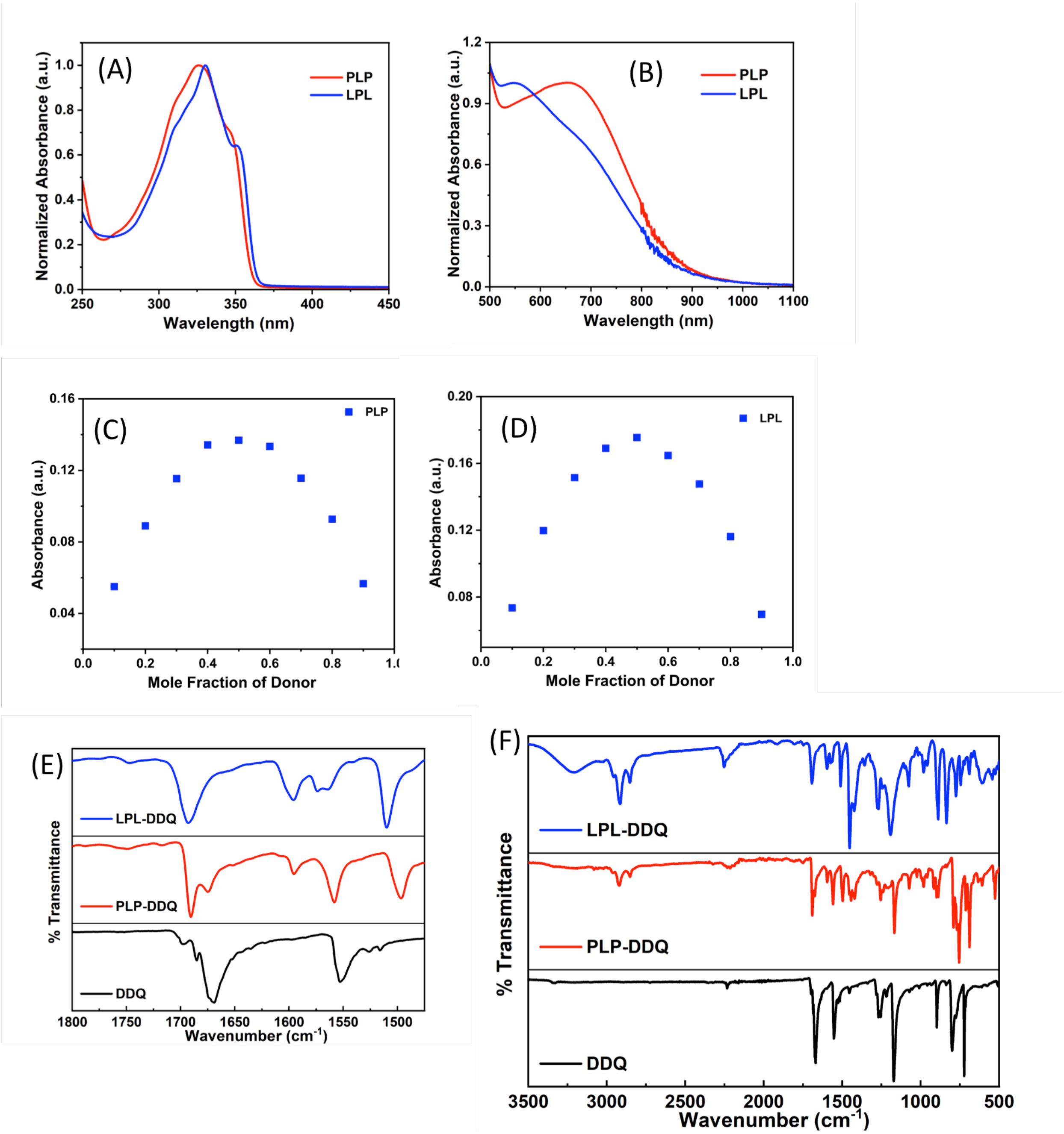

Figure S6. (a) UV-vis absorption spectra of PLP and LPL donors; (b) UV-vis absorption spectra of PLP-DDQ and LPL-DDQ complexes in chloroform; (c) Job's plot of PLP-DDQ and LPL-DDQ complexes; (d and e) ATR-IR spectra of PLP-DDQ and LPL-DDQ complexes.

Donor	Estimated HOMO from CT peak (eV)	Theoretical HOMO (eV)
PPP	-6.207	-5.71
PCP	-6.178	-5.78
CPC	-6.288	-5.77

Table S2. Experimentally estimated and Theoretically calculated HOMOs for all three donors. **Estimated HOMO$_{trimer}$ = LUMO$_{DDQ}$ – λ_{CT}**

The HOMO values of each donor were calculated both experimentally and theoretically. Experimentally, the HOMO values were calculated from the CT UV-Vis peak. Theoretical HOMO values were calculated with DFT.

Computational Methods

Charge Transfer complexes between the designed electron donors with DDQ as an acceptor were computationally modeled using Density Functional Theory (DFT). Geometries

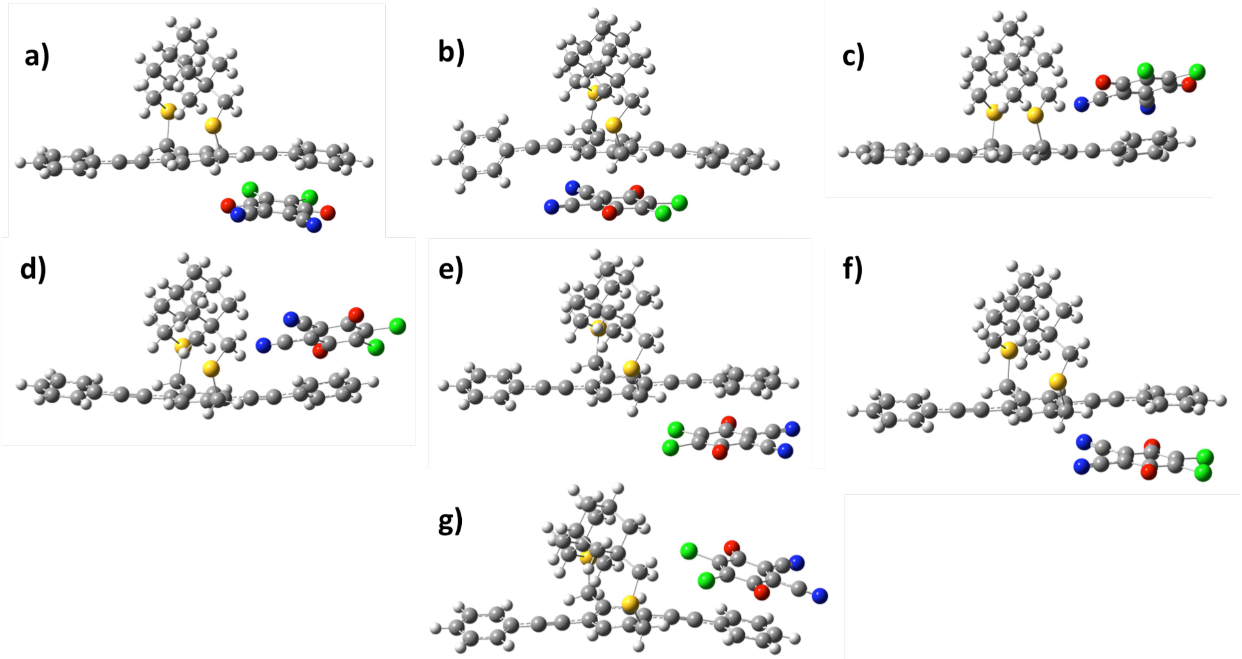

Figure S7. Different geometries explored for PCP-DDQ donor/acceptor complex. All geometries optimized using DFT. . A) PCP-DDQ-1, b) PCP-DDQ-2, c) PCP-DDQ-3, d) PCP-DDQ-4, e) PCP-DDQ-5, f) PCP-DDQ-6, g) PCP-DDQ-7 were optimized using B3LYP/6-311G** with added dispersion correction (GD3BJ) for all systems. Time-dependent density functional theory was done with TD-CAM-B3LYP/6-311G** with added dispersion correction to solve for the excited state properties of the complexes in the gas phase. All geometries investigated for PPP-DDQ system can be seen in Figure 8 in the main text. Figure S7 and Figure S8 show the investigated geometries for the PCP-DDQ and CPC-DDQ complexes, respectively.

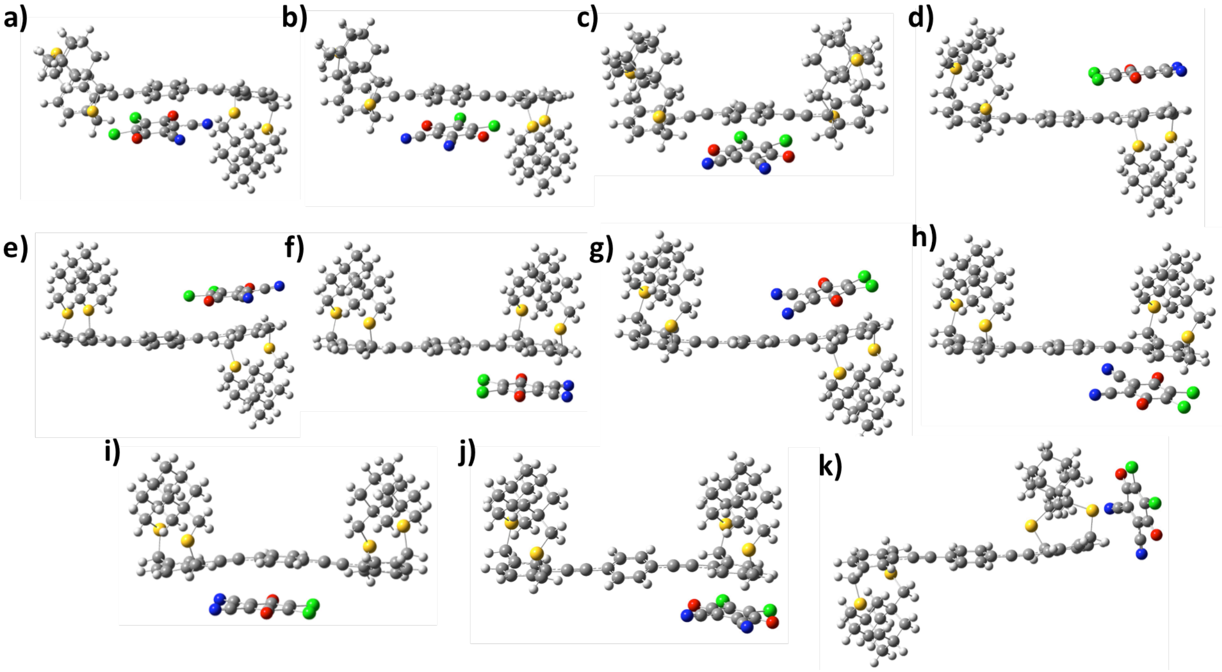

Figure S8. Different geometries explored for CPC-DDQ donor/acceptor complex. All geometries optimized using DFT . A) CPC-DDQ-1, b) CPC-DDQ-2, c) CPC-DDQ-3, d) CPC-DDQ-4, e) CPC-DDQ-5, f) CPC-DDQ-6, g) CPC-DDQ-7, h) CPC-DDQ-8, i) CPC-DDQ-9, j) CPC-DDQ-10, k) CPC-DDQ-11.

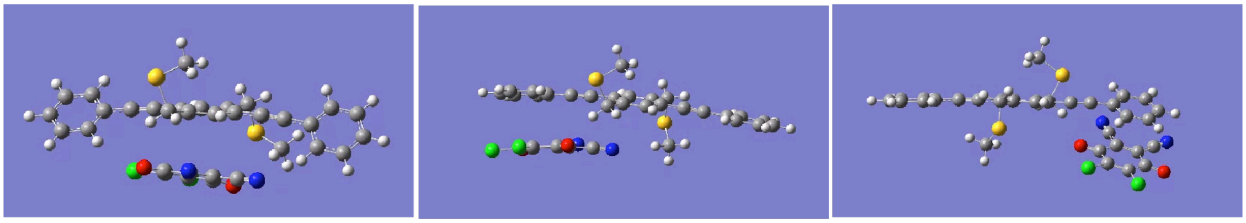

PLP-DDQ-1 PLP-DDQ-2 PLP-DDQ-3

System	BE[a] (kcal/mol)	ΔBE$_r$[b] (kcal/mol)	BF[c]	%Configuration
PLP-DDQ-1	21.6	0	2	64%
PLP-DDQ-2	20.8	0.8	1.05	34%
PLP-DDQ-3	19.2	2.4	0.07	2%

[a]BE (binding energy, BE= -(E$_{complex}$- E$_{donor}$- E$_{DDQ}$); [b]ΔBE$_r$: relative binding energy (ΔBE$_r$=BE (most stable configuration)- BE(complex)); [c]BF: Boltzman factor (BF= g*e$^{-\Delta BEr/RT}$ where g describes the degeneracy of each energy level; ΔBE$_r$: relative binding energy of the complex).

Figure S9. Different geometries explored for PLP-DDQ donor/acceptor complex. All geometries optimized using DFT, A) PLP-DDQ-1, b) PLP-DDQ-2, c) PLP-DDQ-3.

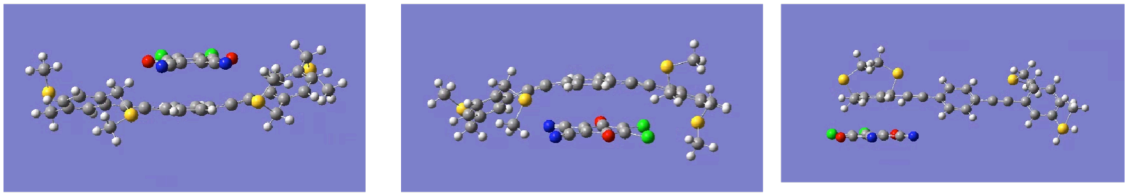

LPL-DDQ-1 LPL-DDQ-2 LPL-DDQ-3

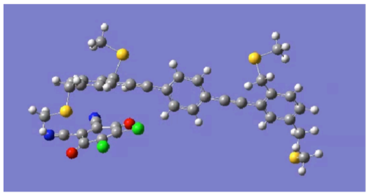

LPL-DDQ-4

System	BE[a] (kcal/mol)	ΔBE$_r$[b] (kcal/mol)	BF[c]	%Configuration
LPL-DDQ-1	22.33	0	2	64%
LPL-DDQ-2	21.91	0.42	1.00	32%
LPL-DDQ-3	20.17	2.16	0.11	3.6%
LPL-DDQ-4	18.84	3.49	0.012	0.4%

[a]BE (binding energy, BE= -(E$_{complex}$- E$_{donor}$- E$_{DDQ}$); [b]ΔBE$_r$: relative binding energy (ΔBE$_r$=BE (most stable configuration)- BE(complex)); [c]BF: Boltzman factor (BF= g*e$^{-\Delta BEr/RT}$ where g describes the degeneracy of each energy level; ΔBE$_r$: relative binding energy of the complex).

Figure S10. Different geometries explored for LPL-DDQ donor/acceptor complex. All geometries optimized using DFT . A) LPL-DDQ-1, b) LPL-DDQ-2, c) LPL-DDQ-3, d) LPL-DDQ-4.

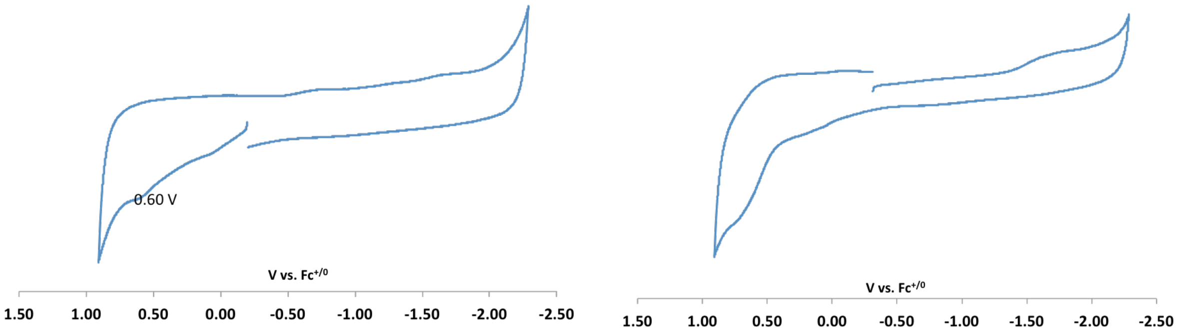

Figure S11: Cyclic voltammograms of PCP (left) and CPC (right).
Experimental conditions: 5mM of trimer was dissolved in THF containing 0.1 M $[^{t}\mathrm{Bu}_4\mathrm{N}][\mathrm{PF}_6]$ as supporting electrolyte. Scan rate: 200 mV/s; working electrode: glassy carbon; reference electrode: Ag/Ag+ referenced to Fc/Fc+; auxiliary electrode: Pt wire.

NMR Spectroscopy

^{1}H NMR spectra for compounds **(±)-9 and (±, meso)-10** recorded in $CDCl_3$. ^{13}C NMR for newly reported compounds **(±)-9** and **(±, meso)-10** recorded in $CDCl_3$ and CD_2Cl_2 respectively.

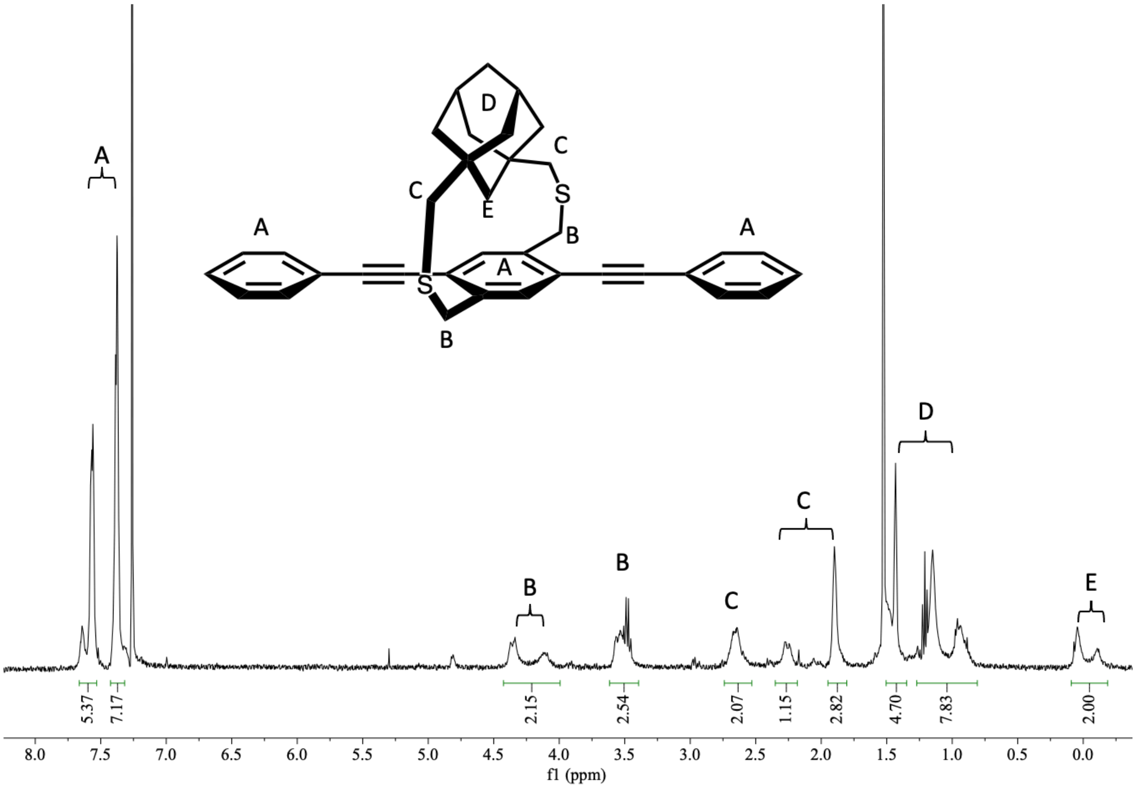

^{1}H NMR (400 MHz, $CDCl_3$) of **(±)-9**

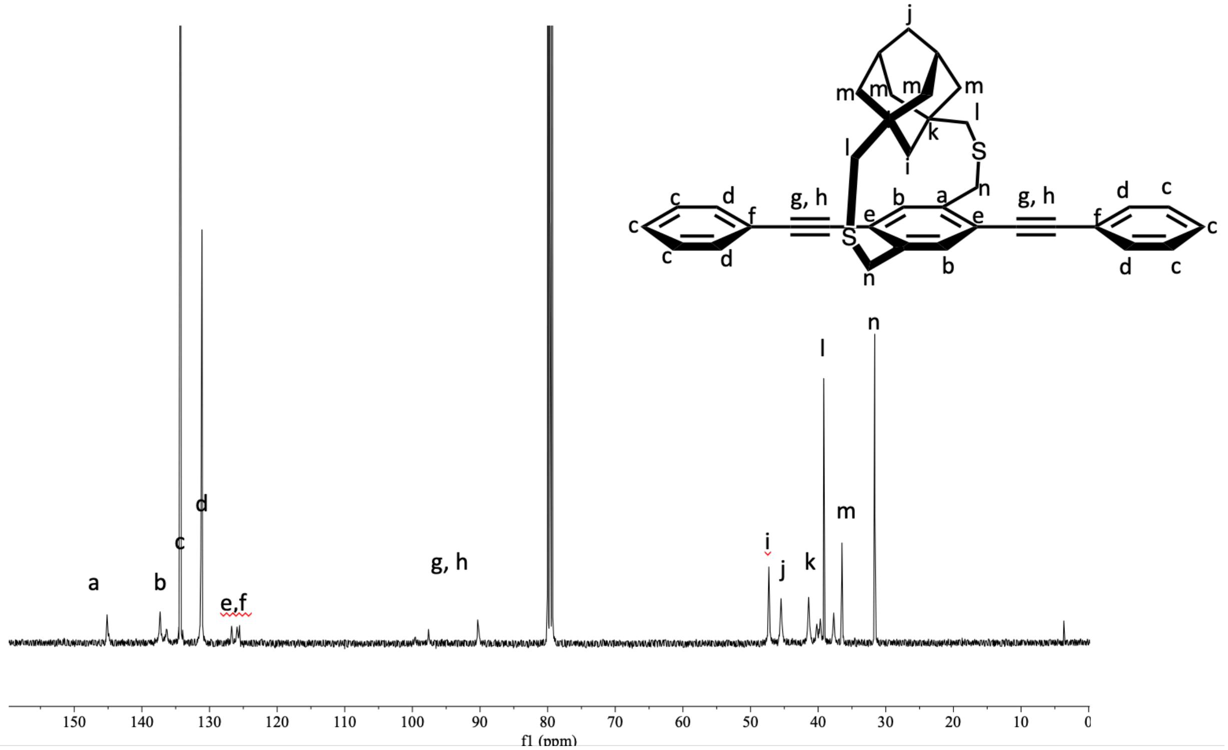

^{13}C NMR (100 MHz, CDCl$_3$) of **(±)-9**

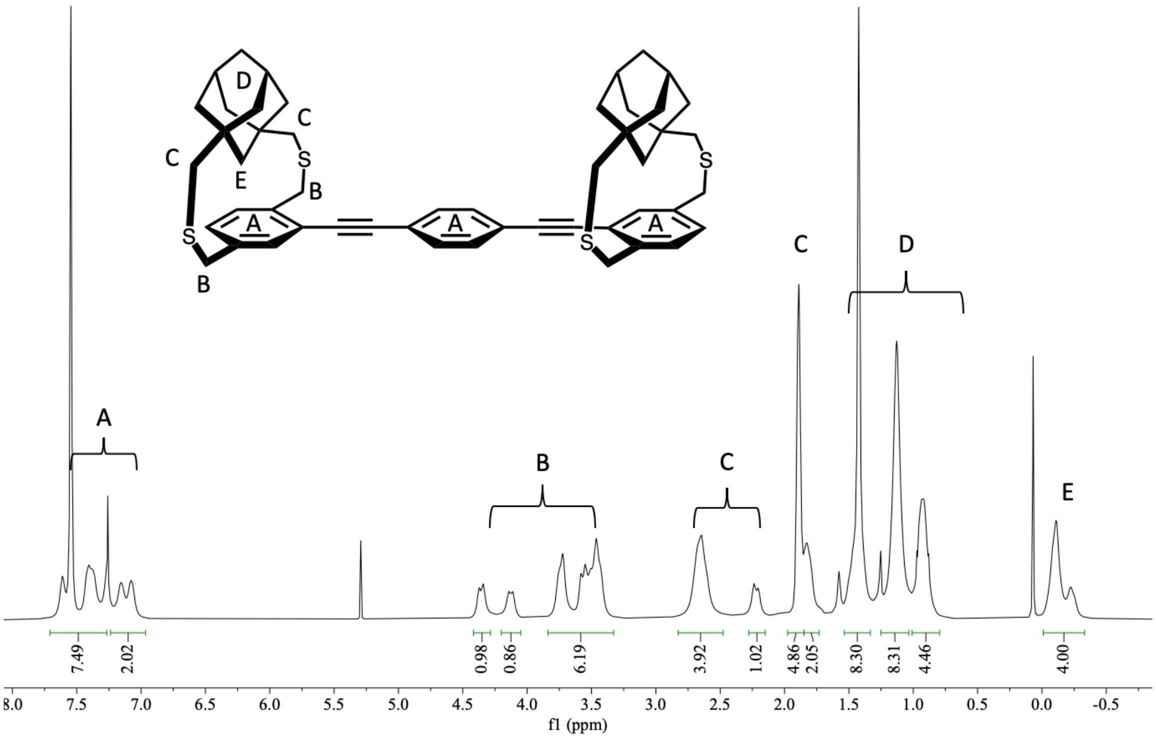

^{1}H NMR (400 MHz, CDCl$_3$) of **(±, meso)-10**

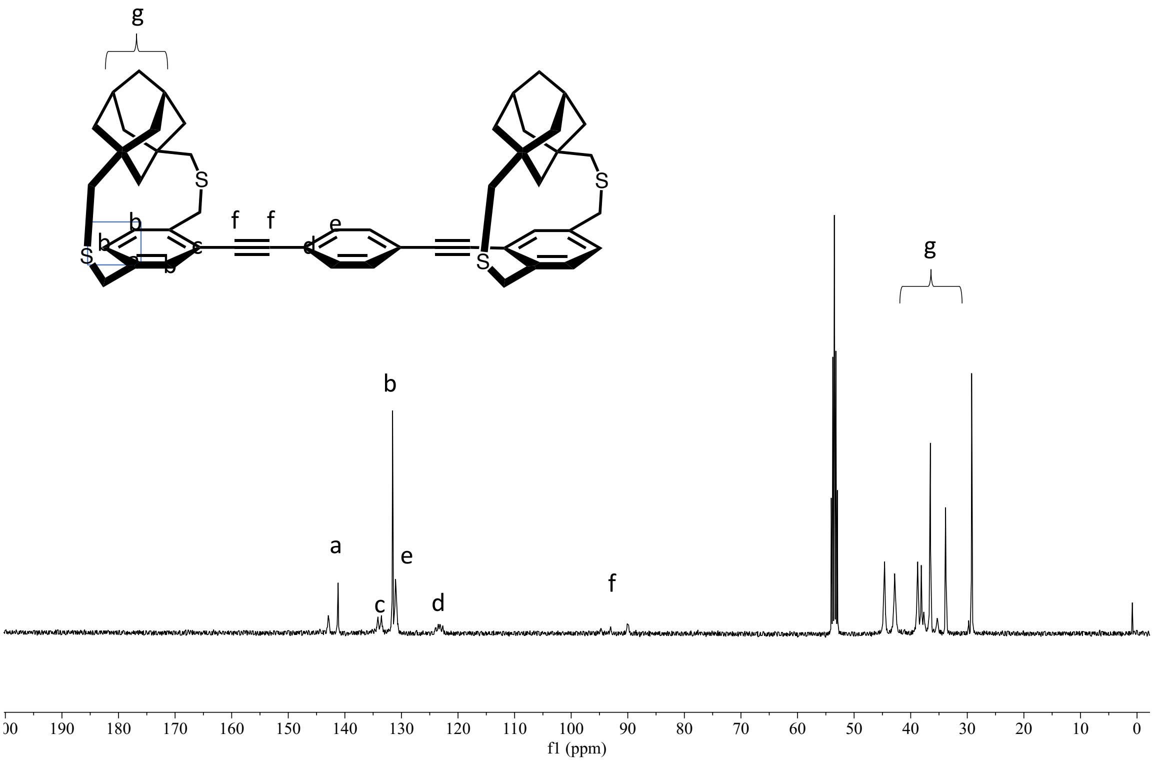

^{13}C NMR (100 MHz, $CDCl_3$) of **(±, meso)-10**

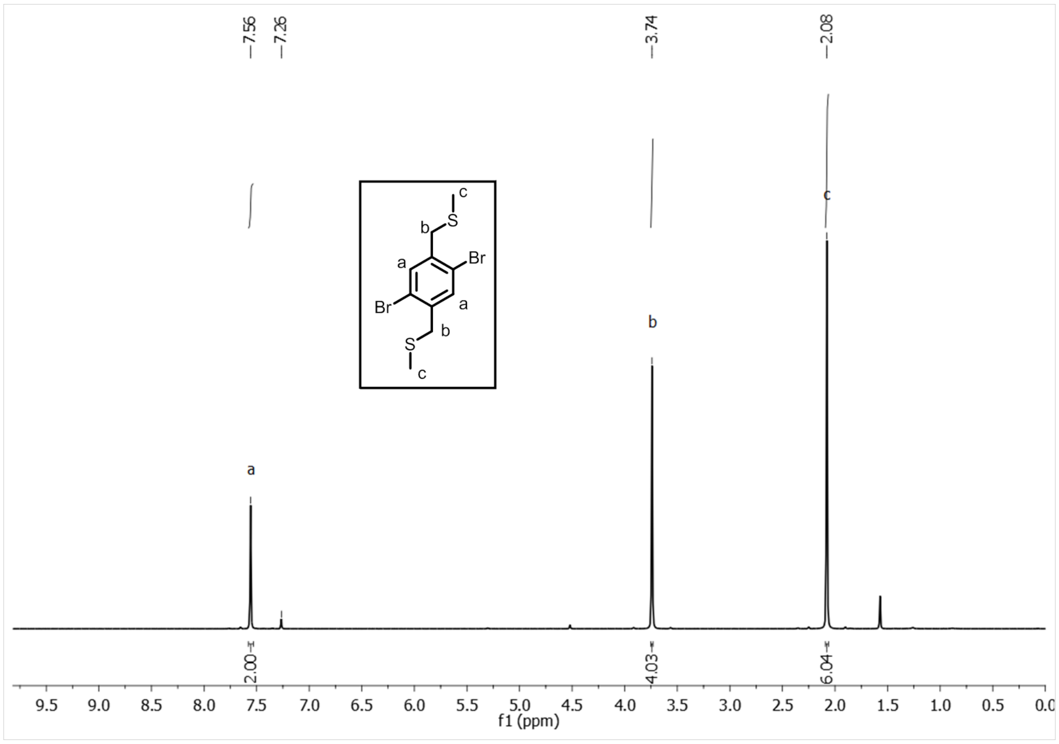

^{1}H NMR (400 MHz, $CDCl_3$) of compound **11**

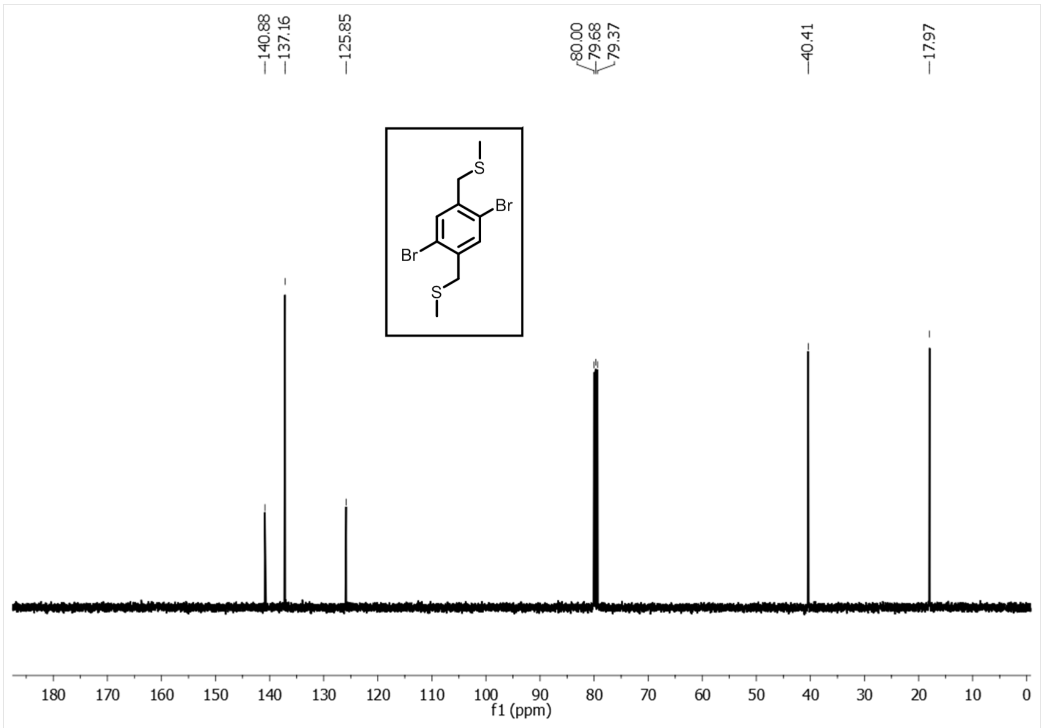

^{13}C NMR (100 MHz, $CDCl_3$) of compound **11**

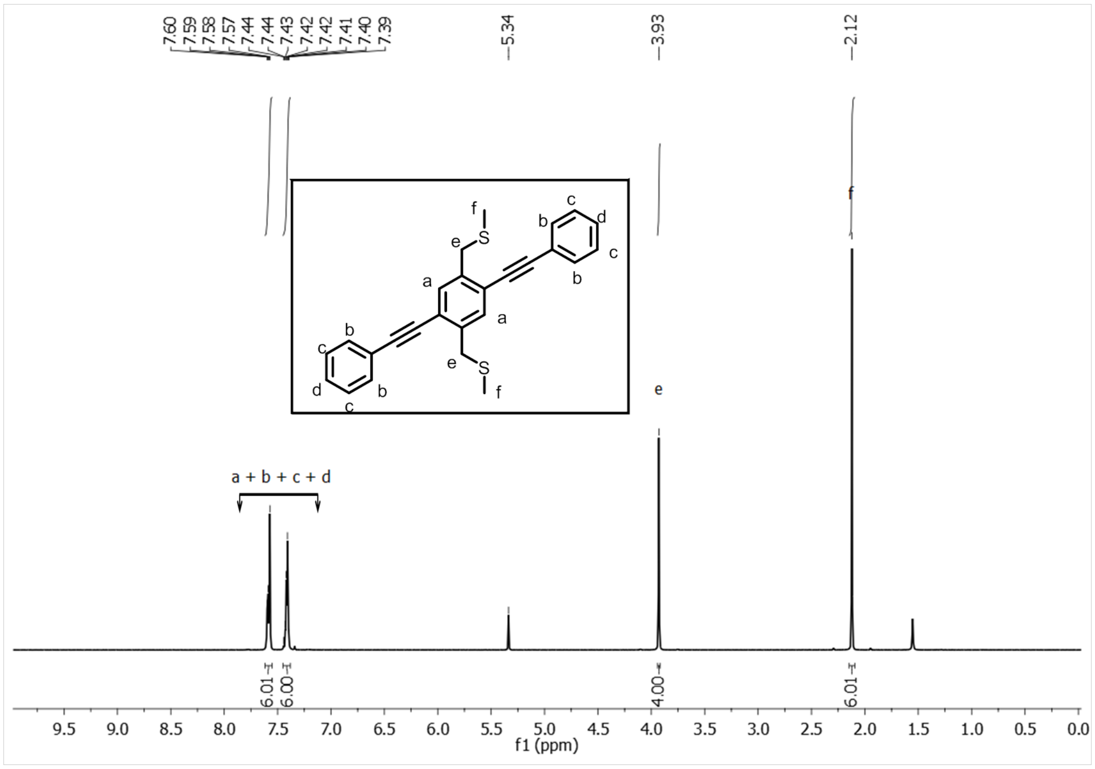

^{1}H NMR (400 MHz, CD_2Cl_2) of compound **12**

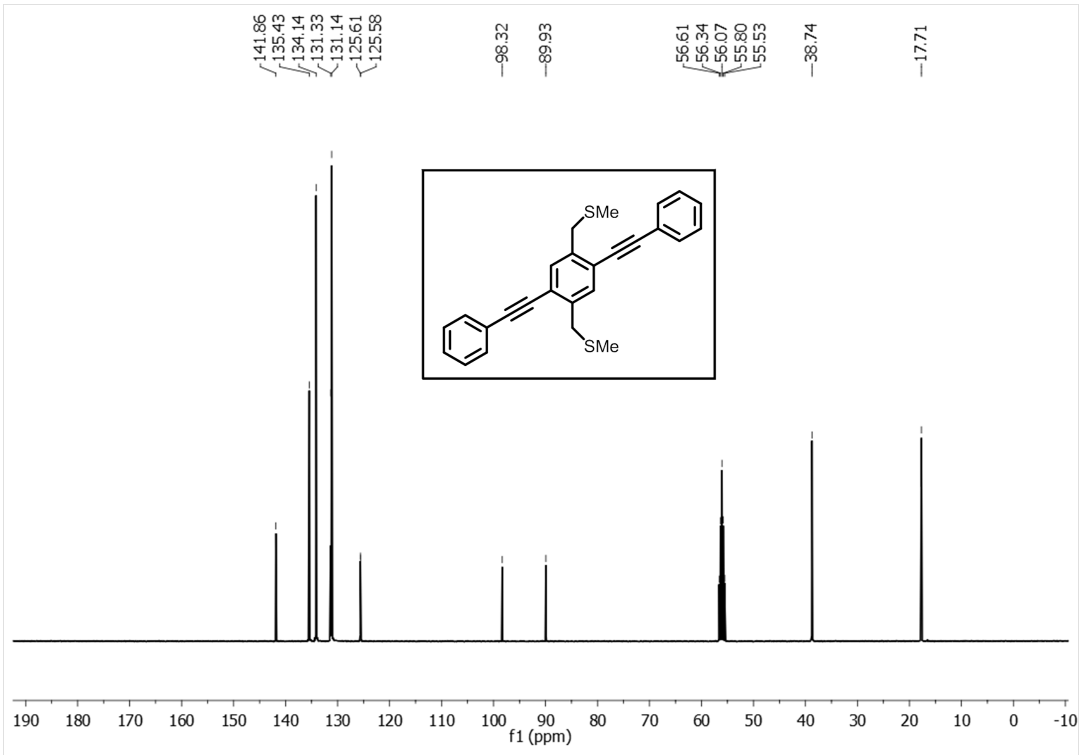

^{13}C NMR (100 MHz, CD_2Cl_2) of compound **12**

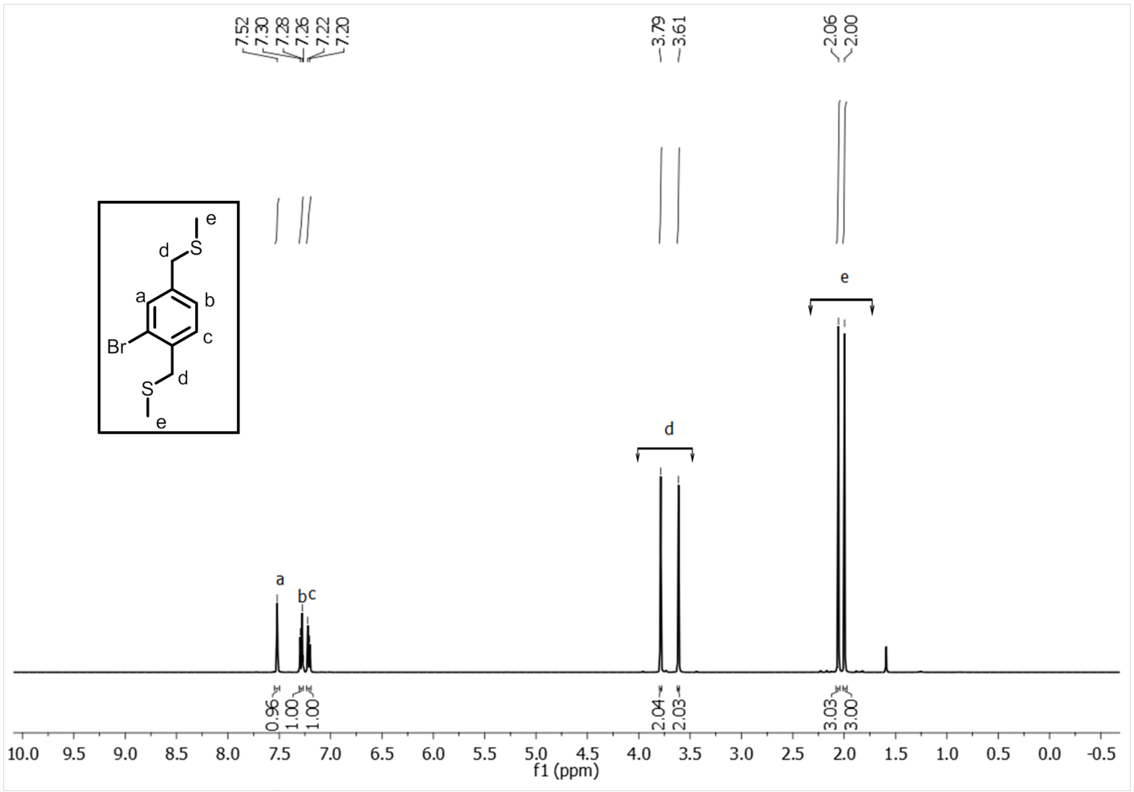

^{1}H NMR (400 MHz, $CDCl_3$) of compound **13**

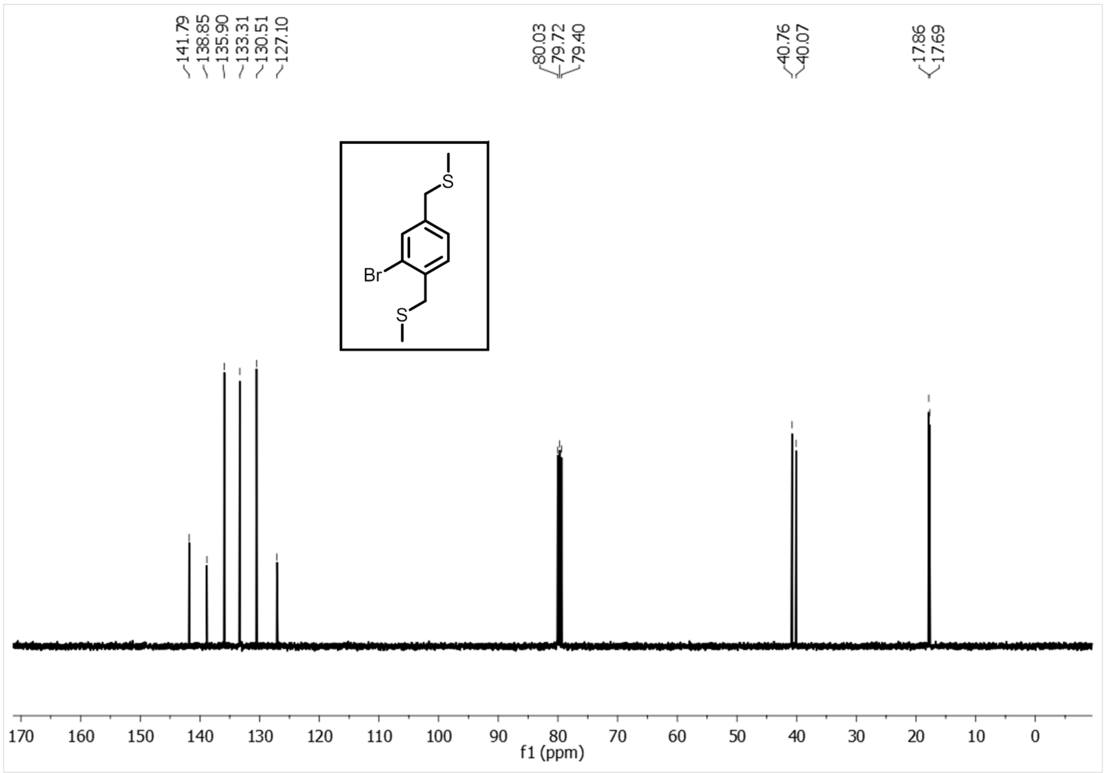

^{13}C NMR (100 MHz, $CDCl_3$) of compound **13**

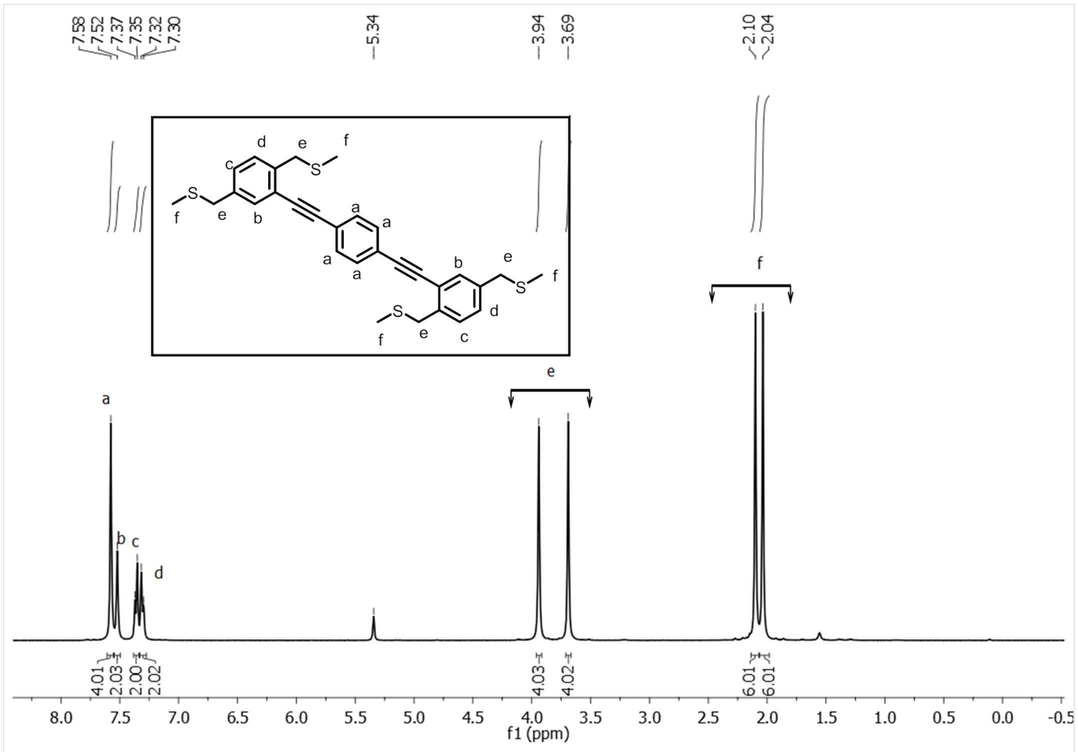

^{1}H NMR (400 MHz, CD_2Cl_2) of compound **14**

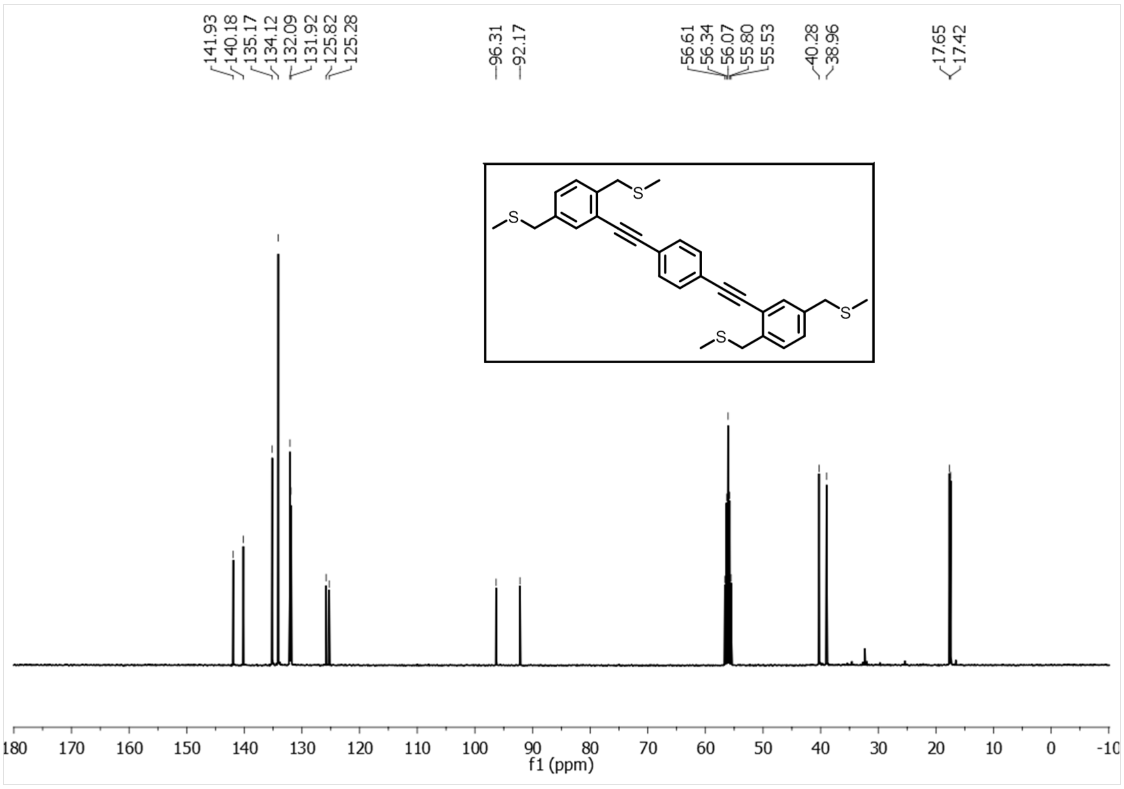

^{13}C NMR (100 MHz, CD_2Cl_2) of compound **14**

References:

1) Lillis, R.; Thomas, M. R.; Mohanan, M.; Gavvalapalli, N., *Macromolecules* **2021,** *54*, 3112-3119.

2) Chaudhuri, S.; Mohanan, M.; Willems, A. V.; Bertke, J. A.; Gavvalapalli, N., *Chem. Sci.* **2019,** *10*, 5976-5982.

3) Das, M. K.; Hameed, F.; Lillis, R.; Gavvalapalli, N., *Mater. Adv.* **2020,** *1*, 2917-2925.

4) Yiying Zhang, Hui Li, Jianhong Chang, Xinyu Guan, Lingxue Tang, Qianrong Fang,* Valentin Valtchev, Yushan Yan, and Shilun Qiu* Small, 2021, **17(22)**, 2006112.

5) Bruker (2016). APEX3, SADABS, SAINT, SHELXTL, XCIF, XPREP. Bruker AXS, Inc., Madison, Wisconsin, USA.

6) Sheldrick, G. M. (2015). Acta Cryst. C71, 3-8.

7) Hubschle, C. B.; Sheldrick, G. M.; Dittrich, B. (2011), J. Appl. Cryst.,44, 1281-1284.